Matrix Decomposition of Precoder Matrix in Orthogonal Precoding for Sidelobe Suppression of OFDM Signals

PAPER

Matrix Decomposition of Precoder Matrix in Orthogonal Precoding for Sidelobe Suppression of OFDM Signals

Hikaru KAWASAKI†, **Masaya OHTA**†a), ***and*** **Katsumi YAMASHITA**†, ***Members***

SUMMARY The spectrum sculpting precoder (SSP) is a precoding scheme for sidelobe suppression of frequency division multiplexing (OFDM) signals. It can form deep spectral notches at chosen frequencies and is suitable for cognitive radio systems. However, the SSP degrades the error rate as the number of notched frequencies increases. Orthogonal precoding that improves the SSP can achieve both spectrum notching and the ideal error rate, but its computational complexity is very high since the precoder matrix is large in size. This paper proposes an effective and equivalent decomposition of the precoder matrix by QR-decomposition in order to reduce the computational complexity of orthogonal precoding. Numerical experiments show that the proposed method can drastically reduce the computational complexity with no performance degradation.

key words: *OFDM, precoding, sidelobe suppression, QR-decomposition, matrix decomposition*

1. Introduction

The advantages of fast data transmission and robustness against multipath fading have led to orthogonal frequency division multiplexing (OFDM) being adopted in several telecommunications technologies. One of the drawbacks associated with the design of OFDM transmitters is that high out-of-band radiation is generated by the high sidelobes of the OFDM signal. A critical issue concerning OFDM-based cognitive radio systems is that the unwanted in-band and out-of-band radiation interferes with adjacent bands. Various methods of sidelobe suppression have been proposed [1]–[9].

N-continuous OFDM [5] is a precoding method to seamlessly connect OFDM symbols up to the high order derivative for sidelobe suppression. Although N-continuous OFDM can suppress out-of-band radiation effectively, it cannot create deep in-band notches for cognitive radio systems. A precoding method for sidelobe suppression that can form spectral notches is the spectrum sculpting precoder (SSP) [6], which satisfies the linear constraints to nullify the power at chosen frequencies. However, the SSP degrades the error rate as the number of notched frequencies increases.

Orthogonal precoding that improves the SSP [7], [8] can achieve both spectrum notching and the ideal error rate; however, the computational complexity of the precoding and decoding is extremely high [9] because of the large size of the precoder matrix.

We have proposed the decomposition of the precoder matrix by singular value decomposition (SVD) that can reduce to a practical amount of complexity [10]. However, it was an approximation method, and was not theoretically guaranteed for any precoder matrices.

This paper proposes a novel matrix decomposition of the precoder matrix using QR-decomposition by Householder reflection in order to reduce the computational complexity in orthogonal precoding. An effective and equivalent decomposition of the precoder matrix can be obtained with a guarantee for significant rank deficiency. Numerical experiments show that the proposed method can drastically reduce the computational complexity with no performance degradation.

2. Orthogonal Precoding of Spectrum Sculpting

In this paper, the OFDM signal is written as

$$s(t) = \sum_{i=0}^{\infty} s_i(t - iT), \tag{1}$$

where $T = T_s + T_g$, T_s is the OFDM symbol duration and T_g is the guard interval length. The i-th OFDM symbol $s_i(t)$ with the cyclic prefix (CP) is calculated by the precoded symbol instead of the data symbol, written as

$$s_i(t) = \sum_{k \in \mathcal{K}} \bar{d}_{i,k} p_k(t) = \mathbf{p}^T(t)\bar{\mathbf{d}}_i, \tag{2}$$

where

$$p_k(t) = e^{j2\pi \frac{k}{T_s} t} I(t), \tag{3}$$
$$\mathbf{p}(t) = [p_{k_0}(t), \dots, p_{k_{K-1}}(t)]^T, \tag{4}$$

the indicator function $I(t) = 1$ for $-T_g \le t < T_s$ and $I(t) = 0$ elsewhere, the modulating symbol $\bar{\mathbf{d}}_i = [\bar{d}_{i,k_0}, \bar{d}_{i,k_1}, \dots, \bar{d}_{i,k_{K-1}}]^T \in \mathbb{C}^{K\times 1}$ is the result of precoding of the data symbol $\mathbf{d}_i = [d_{i,0}, d_{i,1}, \dots, d_{i,D-1}]^T \in \mathbb{C}^{D\times 1}$ containing D information symbols in some finite symbol constellation, $K\ (\ge D)$ is the number of subcarriers, and $\mathcal{K} = \{k_0, \dots, k_{K-1}\}$ are the subcarrier indices. The Fourier transform of (2) is

$$S_i(f) = \sum_{k \in \mathcal{K}} \bar{d}_{i,k} a_k(f) = \mathbf{a}^T(f)\bar{\mathbf{d}}_i, \tag{5}$$

where

Manuscript received August 26, 2017.
Manuscript publicized January 18, 2018.
†The authors are with Department of Electrical and Information Systems, Graduate School of Engineering, Osaka Prefecture University, Sakai-shi, 599-8531 Japan.
a) E-mail: ota@eis.osakafu-u.ac.jp
DOI: 10.1587/transcom.2017EBP3329

$$a_k(f) = Te^{-j\pi(T_s-T_g)(f-\frac{k}{T_s})}\mathrm{sinc}\left(\pi T\left(f-\frac{k}{T_s}\right)\right), \quad (6)$$

is the Fourier transform of $p_k(t)$,

$$\mathbf{a}(f) = [a_{k_0}(f), \ldots, a_{k_{K-1}}(f)]^T, \quad (7)$$

and the cardinal sine is defined as $\mathrm{sinc}(x) = \sin(x)/x$. To render the power spectrum of $s(t)$ zero at the $M\,(\ll K)$ chosen frequencies in $\mathcal{M} = \{f_0, \ldots, f_{M-1}\}$, the SSP scheme [6] satisfies the constraints

$$S_i(f_m) = 0, \;\; m = 0, 1, \ldots, M-1. \quad (8)$$

For (5), the constraints (8) can be cast in matrix form as

$$\mathbf{A}\bar{\mathbf{d}}_i = \mathbf{0}_{M\times 1}, \quad (9)$$

where

$$\mathbf{A} = [\mathbf{a}(f_0), \mathbf{a}(f_1), \ldots, \mathbf{a}(f_{M-1})]^T, \quad (10)$$

embodies the M constrains.

Applying the orthogonal precoding [7] for $D = K - M$, the solution of (9) is expressed as

$$\bar{\mathbf{d}}_i = \mathbf{G}_o\mathbf{d}_i, \quad (11)$$

where the precoder $\mathbf{G}_o \in \mathbb{C}^{K\times(K-M)}$ is a semi-unitary matrix whose columns constitute an orthogonal basis of the null-space for $\mathbf{A}$, that is, it satisfies $\mathbf{A}\mathbf{G}_o = \mathbf{O}_{M\times(K-M)}$ and $\mathbf{G}_o^H\mathbf{G}_o = \mathbf{I}_D$ where $\mathbf{I}_n \in \mathbb{C}^{n\times n}$ denotes an identity matrix. Ref. [7] has determined $\mathbf{G}_o$ as

$$\mathbf{G}_o = \mathbf{V}\mathbf{E}, \quad (12)$$

where $\mathbf{V} \in \mathbb{C}^{K\times K}$ is a unitary matrix obtained from an SVD of $\mathbf{A}$ such as

$$\mathbf{A} = \mathbf{U}\Sigma\mathbf{V}^H, \quad (13)$$

$\mathbf{U} \in \mathbb{C}^{M\times M}$ is a unitary matrix, $\Sigma \in \mathbb{C}^{M\times K}$ is a diagonal matrix containing the singular values of $\mathbf{A}$ in non-increasing order along its diagonal, and the last D columns of $\mathbf{V}$ are collected in $\mathbf{G}_o$ by $\mathbf{E}$, which is denoted by

$$\mathbf{E} = \begin{bmatrix} \mathbf{O}_{M\times D} \\ \mathbf{I}_D \end{bmatrix}. \quad (14)$$

The receiver performs the decoding to obtain the decision variable $\mathbf{r}_i$ for the data symbol $\mathbf{d}_i$ such that

$$\mathbf{r}_i = \mathbf{G}_o^H\tilde{\mathbf{r}}_i, \quad (15)$$

where $\tilde{\mathbf{r}}_i \in \mathbb{C}^K$ is the i-th received OFDM symbol after the CP removal and the frequency-domain equalization (FEQ) in the same way as that of the usual OFDM. Since the precoder matrix $\mathbf{G}_o$ is semi-unitary and satisfies $\mathbf{G}_o^H\mathbf{G}_o = \mathbf{I}_D$, this decoding can invert the transmitter precoding (11) without emphasis of channel characteristics and degradation of the signal-to-noise ratio, and so the data symbol $\mathbf{d}_i$ can be detected accurately.

Ref. [7] shows that the orthogonal precoding has the ideal error rate performance and a sidelobe suppression performance identical to those of the precoding [6]. However, the precoding (11) and decoding (15) each require $KD = K(K-M) \simeq K^2$ multiplications if $K \gg M$, and these are very large [9].

If the rank of $\mathbf{G}_o \in \mathbb{C}^{K\times D}$ is much less than $D = K - M(\simeq K)$, a decomposition of $\mathbf{G}_o$ is a valid choice to tackle this problem since it can be decomposed into a product of smaller matrices. However, the precoder $\mathbf{G}_o$ is a semi-unitary matrix that is essentially full rank (rank$\{\mathbf{G}_o\} \equiv D$), unfortunately.

3. Proposed Method

In order to reduce the computational complexity, we redesign the semi-unitary precoder matrix $\mathbf{G}_o$ in (11) as

$$\mathbf{G}_o = \mathbf{Q}\mathbf{E}, \quad (16)$$

where $\mathbf{Q} \in \mathbb{C}^{K\times K}$ is a unitary matrix obtained from a QR-decomposition of $\mathbf{A}^H \in \mathbb{C}^{K\times M}$ such that

$$\mathbf{A}^H = \mathbf{Q}\mathbf{R}, \quad (17)$$

and $\mathbf{R} \in \mathbb{C}^{K\times M}$ is an upper triangular matrix.

Although $\mathbf{G}_o$ still cannot be decomposed, we then performs an extra QR-decomposition to $\mathbf{Q} - \mathbf{I}_K$ such as

$$\mathbf{Q} - \mathbf{I}_K = \mathbf{C}\mathbf{F}. \quad (18)$$

The reason why $\mathbf{Q}-\mathbf{I}_K$ is considered is that $\mathbf{Q}$ can be trivially reconstructed of $\mathbf{I}_K + \mathbf{C}\mathbf{F}$ after determining $\mathbf{C}$ and $\mathbf{F}$, and we found that the following inequality is always guaranteed for an arbitrary $\mathbf{A}$ (see Appendix):

$$\mathrm{rank}\{\mathbf{Q} - \mathbf{I}_K\} \leq M, \quad (19)$$

which means that $\mathbf{Q} - \mathbf{I}_K \in \mathbb{C}^{K\times K}$ can be decomposed into much smaller matrices for $M \ll K$, that is, into $\mathbf{C} \in \mathbb{C}^{K\times M}$ and $\mathbf{F} \in \mathbb{C}^{M\times K}$.

Substituting (18) into (16), we finally obtain the effective and equivalent decomposition of the semi-unitary matrix $\mathbf{G}_o$ as

$$\mathbf{G}_o = \mathbf{E} + \mathbf{C}\tilde{\mathbf{F}}, \quad (20)$$

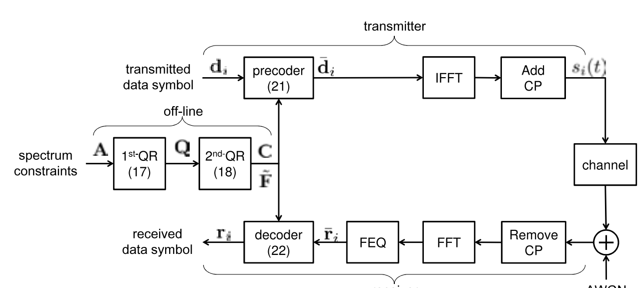

Fig. 1 Block diagram of the proposed method.

where $\tilde{\mathbf{F}} = \mathbf{FE} \in \mathbb{C}^{M\times D}$ is the matrix that collects the last D columns of $\mathbf{F}$.

For (20), the precoding (11) can be rewritten as

$$\bar{\mathbf{d}}_i = \mathbf{E}\mathbf{d}_i + \mathbf{C}\tilde{\mathbf{F}}\mathbf{d}_i, \tag{21}$$

and the decoding (15) can be rewritten as

$$\mathbf{r}_i = \mathbf{E}^H\tilde{\mathbf{r}}_i + \tilde{\mathbf{F}}^H\mathbf{C}^H\tilde{\mathbf{r}}_i. \tag{22}$$

Considering the first terms of (21) and (22) that require no computations in virtue of the property of $\mathbf{E}$ in (14), the proposed precoding (21) and decoding (22) each require $M(K + D) = M(2K - M)$ complex multiplications only for the second terms, instead of the $K(K - M)$ complex multiplications of the conventional orthogonal precoding. Since $M \ll K$ we assumed is based on the fact that practical sidelobe suppression can be achieved by a few $M(\ll K)$ frequencies as shown in Refs. [6] and [7], the computational complexity of the proposed method is much lower than that of the conventional method. Figure 1 show the block diagram of the proposed method using a couple of QR-decompositions.

4. Numerical Experiments

To confirm that the proposed method does not degrade the sidelobe suppression and error rate performances of the conventional method, we firstly conducted numerical experiments based on the conditions in [7]; with QPSK modulation, $T_s = 1/15$ ms, $T_g = 9T_s/128 \simeq 4.69\,\mu$s and the number of subcarriers $K = 600$. In experiments, the SVDs and the QR-decompositions were performed in MATLAB for the conventional and the proposed methods.

Figures 2 and 3 show the power spectral densities (PSDs) of the original OFDM, the OFDM with the windowing method [3], the conventional orthogonal precoding, and the proposed method under the conditions based on those of Figs. 3(a) and (b) in [7], respectively. For the windowing method [3], the raised cosine window was selected as the windowing type, the overlapped region of adjacent

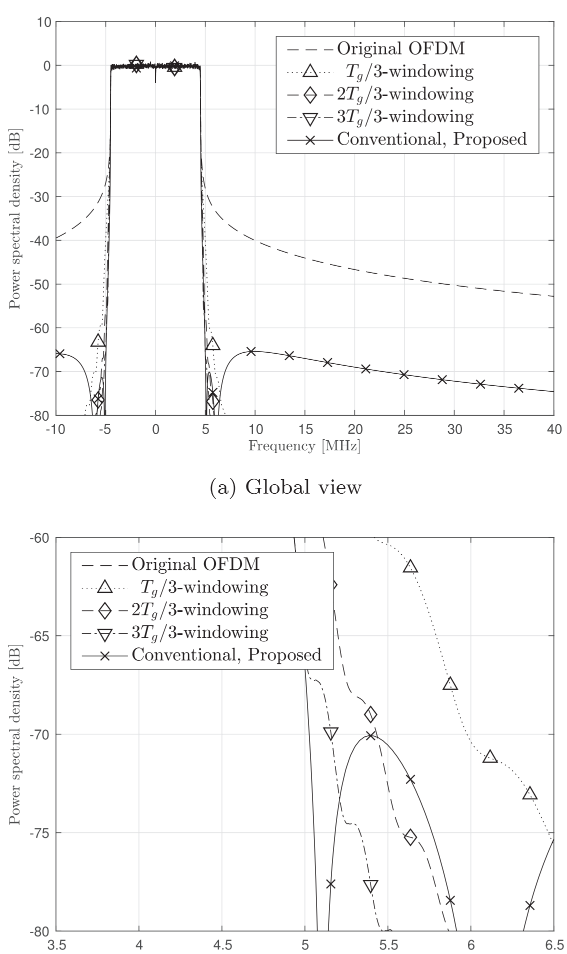

(a) Global view

(b) Enlarged view around 5.0 MHz.

Fig. 2 Power spectral density of original OFDM, OFDM with windowing method, conventional orthogonal precoding, and proposed method; $M = 8$ ($\mathcal{M} = \{\pm 6100\pm 1, \pm 5100\pm 1\}$ kHz) and $K = 600$ ($\mathcal{K} = \{-300, \ldots, -1\} \cup \{1, \ldots, 300\}$).

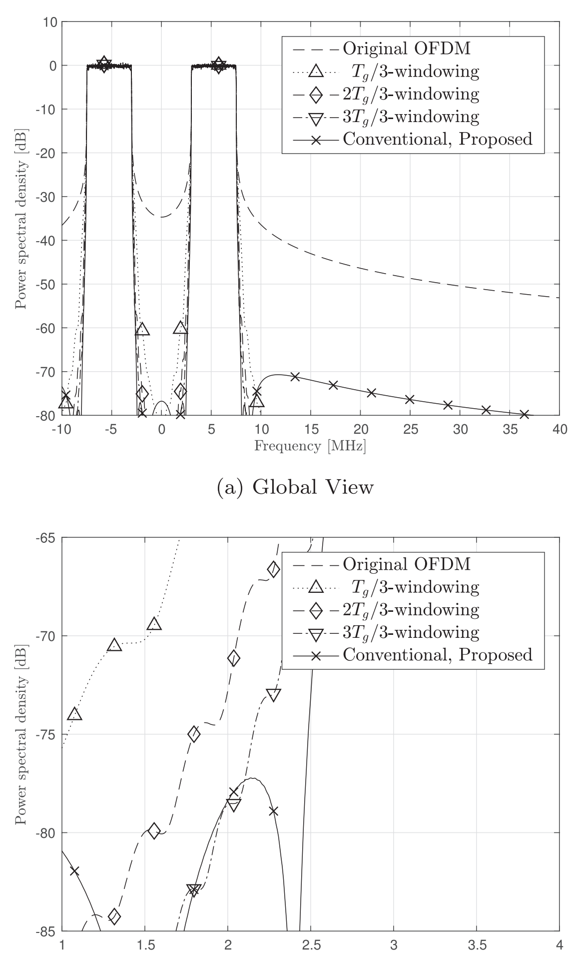

(a) Global View

(b) Enlarged view around 2.5 MHz.

Fig. 3 Power spectral density of original OFDM, OFDM with windowing method, conventional orthogonal precoding, and proposed method; $M = 16$ ($\mathcal{M} = \{\pm 1500\pm 1, \pm 2400\pm 1, \pm 8100\pm 1, \pm 8800\pm 1\}$ kHz) and $K = 600$ ($\mathcal{K} = \{-500, \ldots, -201\} \cup \{201, \ldots, 500\}$).

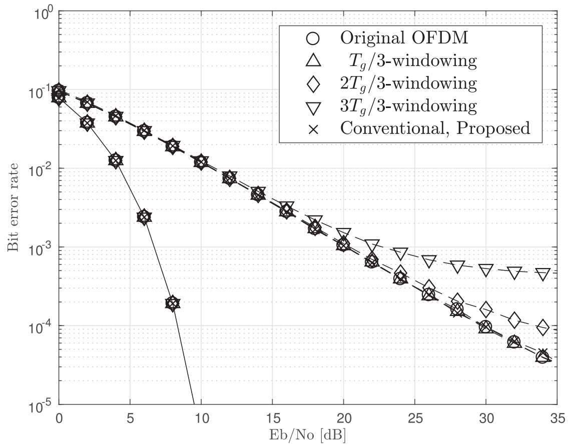

(b) Condition of Fig. 2.

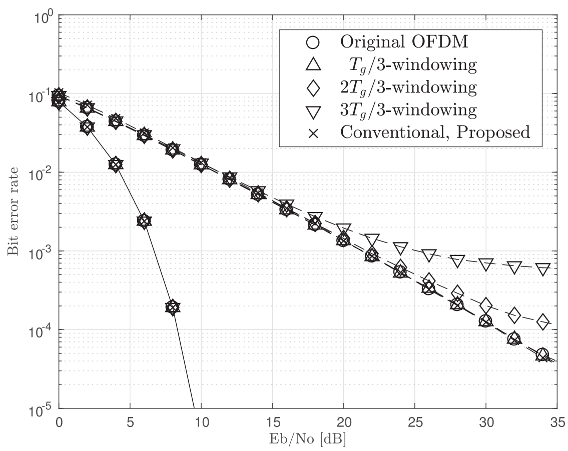

(a) Condition of Fig. 3.

Fig. 4 Bit error rates; solid and dotted lines denote the results in an AWGN channel and multipath Rayleigh fading channel (independent paths of 0, −3, −6 and −9 dB average power at delays 0, 1, 2 and 3 μs [7]), respectively.

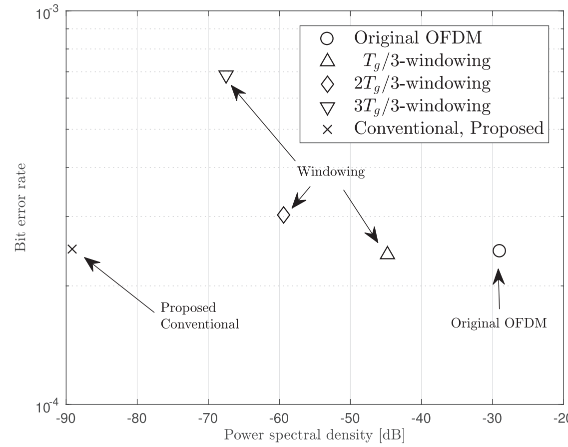

(a) Condition of Fig. 2.

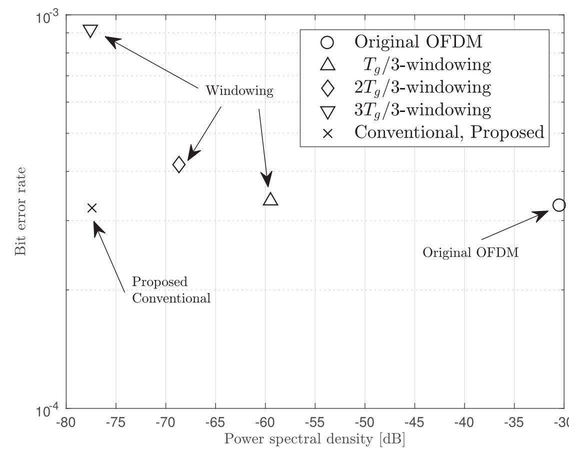

(b) Condition of Fig. 3.

Fig. 5 BER at SNR = 26 dB versus PSD at near band-edge; (a) and (b) see the PSDs at 5.1 MHz and at 2.1 MHz, respectively.

OFDM symbols was held in each head of guard intervals, and the length of the overlapped region was referred to as the windowing length in this paper. The sidelobe suppression performance of the proposed method is identical to that of the conventional orthogonal precoding due to its equivalent decomposition. The enlarged views shows that the conventional and the proposed methods can decay the PSD more rapidly near band-edge than the windowing method. Figure 4 shows the bit error rates (BERs) in an additive white Gaussian noise (AWGN) channel and in a multipath Rayleigh fading channel whose maximum delay time in fading channel did not excess the length of CP in the guard interval on the assumption of the perfect channel estimation and the use of the one-tap FEQ. In the AWGN channel, the windowing method and the orthogonal precoding are identical to the original OFDM in terms of error rate performance. On the other hand in the fading channel, the windowing method degraded the error rate as the windowing length increased. In the windowing method, the overlapped region in the head of guard interval damaged a part of CP to combat multipath fading and thus the error rate became inferior to that of the original OFDM when the maximum delay time in multipath environment is longer. In contrast, the proposed method certainly coincided with the original OFDM due to a complete CP in BER performance.

Figure 5 plots the BER versus the PSD for the comparison of the proposed method and the windowing method. To rapidly suppress the PSD near band-edge, the windowing method required to increase the windowing length but it degraded the error rate severely. On the other hand, the conventional and the proposed methods can achieve both a fast decay of the PSD and a practical error rate performance. For example, Fig. 5(b) shows that the error rate of the proposed method was 1/3 lower than that of the T_g-length windowing method at the same PSD.

We then evaluated the computational complexity of the proposed method compared with that of the conventional orthogonal precoding under the conditions of Figs. 2 and 3. Table 1 shows the computational complexity of the proposed method in the complex multiplications compared with

Table 1 Comparison of computational complexity of precoding/decoding in complex multiplications.

Condition (K, M)	Fig. 2 (600, 8)	Fig. 3 (600, 16)
Conventional [7] $(K(K-M))$	355, 200 (100%)	350, 400 (100%)
Proposed $(M(2K-M))$	9, 536 (2.7%)	18, 944 (5.4%)

the conventional method. The conventional orthogonal precoding has an obvious enormous computational complexity. In contrast, the proposed method can drastically reduce the computational complexity.

From these results, it is verified that the proposed method has excellent performances identical to those of the conventional orthogonal precoding with much lower computational complexity in virtue of the effective and equivalent decomposition of the precoder.

5. Conclusions

This paper has proposed a matrix decomposition of the semi-unitary precoder matrix in the orthogonal precoding in order to reduce the computational complexity. Using QR-decomposition by Householder reflection, the rank decomposition can be obtained with a guarantee for significant computational complexity reduction, and this leads to the effective and equivalent decomposition of the precoder matrix. Numerical experiments have shown that the proposed method does not degrade the performance and can reduce the computational complexity drastically for both precoding and decoding, e.g., to 2.7%, compared with the conventional orthogonal precoding.

In future work, we will investigate the adoption of the proposed method in systems where occupied band is dynamically assigned, for example, OFDMA systems. Since the proposed method requires two QR-factorizations to recalculate the precoder, a novel techniques to more reduce the computational complexity should be developed for such systems.

Acknowledgements

This work was supported by JSPS KAKENHI Grant Number JP16J07452, JP15K06074.

References

[1] S. Brandes, I. Cosovic, and M. Schnell, "Reduction of out-of-band radiation in OFDM systems by insertion of cancellation carriers," IEEE Commun. Lett., vol.10, no.6, pp.420–422, June 2006.

[2] I. Cosovic, S. Brandes, and M. Schnell, "Subcarrier weighting: A method for sidelobe suppression in OFDM systems," IEEE Commun. Lett., vol.10, no.6, pp.444–446, June 2006.

[3] T. Weiss, J. Hillenbrand, A. Krohn, and F.K. Jondral, "Mutual interference in OFDM-based spectrum pooling system," Proc. IEEE Veh. Technol. Conf., vol.4, pp.1873–1877, May 2004.

[4] H.A. Mahmoud and H. Arslan, "Sidelobe suppression in OFDM-based spectrum sharing systems using adaptive symbol transition," IEEE Commun. Lett., vol.12, no.2, pp.133–135, Feb. 2008.

[5] J. van de Beek, and F. Berggren, "N-continuous OFDM," IEEE Commun. Lett., vol.13, no.1, pp.1–3, Jan. 2009.

[6] J. van de Beek, "Sculpting the multicarrier spectrum: A novel projection precoder," IEEE Commun. Lett., vol.13, no.12, pp.881–883, 2009.

[7] J. van de Beek, "Orthogonal multiplexing in a subspace of frequency well-localized signals," IEEE Commun. Lett., vol.14, no.10, pp.882–884, 2010.

[8] M. Ma, X. Huang, B. Jiao, and Y.J. Guo, "Optimal orthogonal precoding for power leakage suppression in DFT-based systems," IEEE Trans. Commun., vol.59, no.3, pp.844–853, 2011.

[9] R. Kumar and A. Tyagi, "Computationally efficient mask-compliant spectral precoder for OFDM cognitive radio," IEEE Trans. Cogn. Commun. Netw., vol.2, no.1, pp.15–23, 2016.

[10] H. Kawasaki, M. Ohta, and K. Yamashita, "Computational complexity reduction of orthogonal precoding for sidelobe suppression of OFDM signal," The 21th Asia-Pacific Conference on Communications (APCC 2015), pp.460–463, Kyoto, Oct. 2015.

[11] B. Sudipto and R. Anindya, Linear Algebra and Matrix Analysis for Statistics, 1st ed., Texts in Statistical Science, Chapman and Hall/CRC, 2014.

[12] V.C. Venkaiah, V. Krishna, and A. Paulraj, "Householder transformation in C^m," Digital Signal Process., vol.3, no.4, pp.266–277, 1993.

[13] G.H. Golub and C.F. Van Loan, Matrix Computations, pp.374–426, Johns Hopkins University Press, Baltimore, MD, USA, 1996.

Appendix

We have proven the following Theorem:

Theorem 1. *If an arbitrary matrix* $\mathbf{B} \in \mathbb{C}^{K\times M}$ *with* $K > M$ *is decomposed into* $\mathbf{B} = \mathbf{QR}$ *of a unitary matrix* $\mathbf{Q} \in \mathbb{C}^{K\times K}$ *and an upper triangular matrix* $\mathbf{R} \in \mathbb{C}^{K\times M}$ *by a QR-decomposition using Householder reflection, then*

$$\operatorname{rank}\{\mathbf{Q} - \mathbf{I}_K\} \le M, \tag{A·1}$$

is satisfied.

Before presenting a proof of Theorem 1, some fundamental lemmas are noted.

Lemma 1. *Let* $\mathbf{X} \in \mathbb{C}^{n\times n}$ *and* $\mathbf{Y} \in \mathbb{C}^{n\times m}$ *be arbitrary matrices. Then*

$$\operatorname{rank}\{\mathbf{XY}\} \le \operatorname{rank}\{\mathbf{X}\}, \tag{A·2}$$
$$\operatorname{rank}\{\mathbf{XY}\} \le \operatorname{rank}\{\mathbf{Y}\}, \tag{A·3}$$
$$\operatorname{rank}\{\mathbf{XY}\} \le \operatorname{rank}\{\mathbf{X}\} + \operatorname{rank}\{\mathbf{Y}\}, \tag{A·4}$$
$$\operatorname{rank}\{\mathbf{X} - \mathbf{I}_n\} = \operatorname{rank}\left\{\mathbf{X}^H - \mathbf{I}_n\right\}, \tag{A·5}$$

are satisfied.

Proof. see [11]. □

Lemma 2. *Let* $\mathbf{X}_0, \mathbf{X}_1, \ldots, \mathbf{X}_{M-1} \in \mathbb{C}^{n\times n}$ *be arbitrary square matrices. Then*

$$\operatorname{rank}\left\{\prod_{m=0}^{M-1} \mathbf{X}_m - \mathbf{I}_n\right\} \le \sum_{m=0}^{M-1} \operatorname{rank}\{\mathbf{X}_m - \mathbf{I}_n\}, \tag{A·6}$$

is satisfied.

Proof. Noting that

$$\prod_{m=0}^{M-1} \mathbf{X}_m - \mathbf{I}_n = \mathbf{X}_0 - \mathbf{I}_n + \mathbf{X}_0\left(\prod_{m=1}^{M-1} \mathbf{X}_m - \mathbf{I}_n\right), \quad \text{(A· 7)}$$

and Lemma 1, we obtain

$$\begin{aligned}
&\text{rank}\left\{\prod_{m=0}^{M-1} \mathbf{X}_m - \mathbf{I}_n\right\} \\
&\le \text{rank}\left\{\mathbf{X}_0 - \mathbf{I}_n\right\} + \text{rank}\left\{\mathbf{X}_0\left(\prod_{m=1}^{M-1} \mathbf{X}_m - \mathbf{I}_n\right)\right\} \\
&\le \text{rank}\left\{\mathbf{X}_0 - \mathbf{I}_n\right\} + \text{rank}\left\{\prod_{m=1}^{M-1} \mathbf{X}_m - \mathbf{I}_n\right\} \\
&\le \sum_{m=0}^{1} \text{rank}\left\{\mathbf{X}_m - \mathbf{I}_n\right\} + \text{rank}\left\{\prod_{m=2}^{M-1} \mathbf{X}_m - \mathbf{I}_n\right\} \\
&\le \cdots \le \sum_{m=0}^{M-1} \text{rank}\left\{\mathbf{X}_m - \mathbf{I}_n\right\}. \qquad \text{(A· 8)}
\end{aligned}$$

□

Lemma 3. *Let* $\mathbf{a} \in \mathbb{C}^n$ *and* $\mathbf{b} \in \mathbb{C}^n$ *be given vectors and* $\tilde{\mathbf{H}}_{(n)} \in \mathbb{C}^{n\times n}$ *be a Householder matrix satisfying* $\tilde{\mathbf{H}}_{(n)}\mathbf{b} = \mathbf{a}$. *Then,*

$$\text{rank}\left\{\tilde{\mathbf{H}}_{(n)} - \mathbf{I}_n\right\} = 1, \quad \text{(A· 9)}$$

is satisfied.

Proof. We let $\mathbf{w} = \mathbf{b} - \mathbf{a} \in \mathbb{C}^n$. Then, from [12], $\tilde{\mathbf{H}}_{(n)}$ is written as

$$\tilde{\mathbf{H}}_{(n)} = \mathbf{I}_n - (1 + w)\mathbf{w}\mathbf{w}^H, \quad \text{(A· 10)}$$

where $w = (\mathbf{w}^H\mathbf{a})^H/\mathbf{w}^H\mathbf{a} \neq -1$ and $|w| = 1$. Noting that $\text{rank}\left\{\mathbf{w}\mathbf{w}^H\right\} = \text{rank}\left\{\mathbf{w}\right\}$ is shown in [11], we prove (A· 9) as

$$\begin{aligned}
\text{rank}\left\{\tilde{\mathbf{H}}_{(n)} - \mathbf{I}_n\right\} &= \text{rank}\left\{-(1+w)\mathbf{w}\mathbf{w}^H\right\} \\
&= \text{rank}\left\{\mathbf{w}\right\} = 1. \qquad \text{(A· 11)}
\end{aligned}$$

□

Using the above Lemmas, we can prove Theorem 1 as follows.

Proof. From [13], $\mathbf{Q}$ and $\mathbf{R}$ can be written as

$$\mathbf{Q} = (\mathbf{H}_{M-1}\mathbf{H}_{M-2}\cdots\mathbf{H}_0)^H = \prod_{m=0}^{M-1} \mathbf{H}_m^H, \quad \text{(A· 12)}$$

$$\mathbf{R} = \mathbf{H}_{M-1}\mathbf{H}_{M-2}\cdots\mathbf{H}_0\mathbf{B} = \mathbf{B}_M = \mathbf{Q}^H\mathbf{B}, \quad \text{(A· 13)}$$

where $\mathbf{H}_0, \mathbf{H}_1, \ldots, \mathbf{H}_{M-1} \in \mathbb{C}^{K\times K}$ are the unitary matrices, which is denoted by

$$\mathbf{H}_m = \begin{bmatrix} \mathbf{I}_m & \mathbf{O}_{m\times(K-m)} \\ \mathbf{O}_{(K-m)\times m} & \tilde{\mathbf{H}}_{(K-m)} \end{bmatrix}, \quad \text{(A· 14)}$$

and $\tilde{\mathbf{H}}_{(K-m)} \in \mathbb{C}^{(K-m)\times(K-m)}$ are the Householder matrices defined in a similar way to (A· 10) for $m \geq 0 \in \mathbb{N}$. For (A· 12), we can obtain

$$\begin{aligned}
\text{rank}\left\{\mathbf{Q} - \mathbf{I}_K\right\} &= \text{rank}\left\{\prod_{m=0}^{M-1} \mathbf{H}_m^H - \mathbf{I}_K\right\} \\
&\le \sum_{m=0}^{M-1} \text{rank}\left\{\mathbf{H}_m^H - \mathbf{I}_K\right\} \\
&= \sum_{m=0}^{M-1} \text{rank}\left\{\mathbf{H}_m - \mathbf{I}_K\right\}, \qquad \text{(A· 15)}
\end{aligned}$$

from Lemmas 1 and 2. The definition (A· 14) and Lemma 3 lead to

$$\begin{aligned}
&\text{rank}\left\{\mathbf{H}_m - \mathbf{I}_K\right\} \\
&= \text{rank}\left\{\begin{bmatrix} \mathbf{O}_{m\times m} & \mathbf{O}_{m\times(K-m)} \\ \mathbf{O}_{(K-m)\times m} & \tilde{\mathbf{H}}_{(K-m)} - \mathbf{I}_{K-m} \end{bmatrix}\right\} \\
&= \text{rank}\left\{\tilde{\mathbf{H}}_{(K-m)} - \mathbf{I}_{K-m}\right\} \\
&= 1, \qquad \text{(A· 16)}
\end{aligned}$$

and thus we obtain

$$\text{rank}\left\{\mathbf{Q} - \mathbf{I}_K\right\} \le \sum_{m=0}^{M-1} \text{rank}\left\{\mathbf{H}_m - \mathbf{I}_K\right\} = M. \quad \text{(A· 17)}$$

□

Hikaru Kawasaki received the B.E. degree and the M.E degree from Osaka Prefecture University in 2013 and 2015, respectively, He received Ph.D from Osaka Prefecture University in 2017 through a grade skipping. He is primarily pursuing research related to signal processing for OFDM systems. He is a member of IEEE and IEICE.

Masaya Ohta received a B.E. degree from Osaka Prefecture University in 1991, completed the first and second halves of the doctoral program in 1993 and 1996. He became a lecturer at Osaka Electro-communication University in 1996, a lecturer at the Graduate School of Engineering, Osaka Prefecture University in 2002, an associate professor in 2012. He has been a professor at the Graduate School of Humanities and Sustainable System Sciences. He is mostly engaged in research on information communication systems and virtual/augmented reality systems. He holds a D.Eng. degree, and is a member of IEEE, IEEJ, and the Information Processing Society.

Katsumi Yamashita received the B.E. degree from Kansai University, the M.E. degree from Osaka Prefecture University and the Dr.Eng. degree from Osaka University in 1974, 1976 and 1985, respectively, all in electrical engineering. In 1982, he became an assistant professor in University of the Ryukyus, where he was a professor in 1991. Now he is a professor and the director of I.I.C. lab. His current interests are in digital communication, digital signal processing. Dr. Yamashita is a member of the IEEE, and IEICE, IEEJ.